Coil detection of optically generated magnons in MnF_2:Er^{3+}

G. J. Jongerden, A. F. M. Arts, J. I. Dijkhuis, and H. W. de Wijn
Fysisch Laboratorium, Rijksuniversiteit Utrecht, P.O. Box 80.000, 3508 TA Utrecht, The Netherlands
(Received 24 May 1988; revised manuscript received 14 November 1988)

Nonzero-wave-vector magnons in MnF_2 are generated by pulsed optical excitation of the upper $^4F_{9/2}(1)$ level of 0.01-at. % Er^{3+} centers followed by decay to the lower $^4F_{9/2}(1)$ level. Their relaxation is subsequently detected via the voltage the associated changes of the magnetization induce in a coil around the specimen. The magnon intrinsic lifetime appears to be at least 1 μs. The Er^{3+} spin-magnon relaxation time, which scales approximately inversely with the density of magnon states, drops to 30 ns at wave vectors 10% out towards the Brillouin-zone boundary.

I. INTRODUCTION

In a previous paper,[1] it was demonstrated that selective optical excitation of Er^{3+} centers into the upper component of the Zeeman-split $^4F_{9/2}(1)$ Kramers doublet and the emission of a resonant magnon in the subsequent decay to the lower doublet level is an effective means of generating magnons of nonzero wave vector in antiferromagnets, notably MnF_2. The magnons produced, belonging to a single branch, chiefly reside on one sublattice, namely the one with the downward moments. They, therefore, give rise to a macroscopic magnetization. This provides, via a voltage induced in a pickup coil, direct access to the magnon occupation as it evolves with time.

Below, the usefulness of time-resolved coil detection is explored. The method is employed to see the magnon occupation develop as a result of, on the one hand, feeding by spin-magnon relaxation and, on the other hand, decay by thermalization. The experiments provide, with a time resolution of few nanoseconds only, the dependence of spin-magnon relaxation upon moving away from the center of the Brillouin zone. As it turns out, the dependence on the magnon energy is dominated by the density of states. This is confirmed by a calculation based on an Er^{3+}-Mn^{2+} interaction of general form. The magnons are further found to be long-lived on a microsecond time scale.

In addition, coil detection is utilized in a spectroscopic investigation of the $^4I_{15/2}(1)$-$^4F_{9/2}(1)$ transition of Er^{3+} in MnF_2. Here, the induction voltage, monitored as a function of the laser frequency, allows an unambiguous assignment of the various Zeeman components of the optical transition to the magnetic sublattices.

II. EXPERIMENT

Pulsed optical excitation into the $^4F_{9/2}(1)$ levels of Er^{3+} in MnF_2 was performed by use of an excimer-pumped dye laser, generating light pulses of 10-ns duration, 100-kW peak power, and 0.3-cm^{-1} spectral width. The laser light, nearly linearly polarized and propagated along [001], was focused to a waist of 1 mm diam in the crystal. The specimen, a crystal of MnF_2 containing 0.01 at. % Er^{3+} according to atomic absorption spectroscopy, has dimensions $1.5\times2.0\times12.0$ mm^3, with the [001] axis pointing along the longest dimension. It was immersed in liquid helium held at 1.5 K. A 25-turn coil was wrapped around the sample such as to be sensitive to magnetization changes along [001]. The coil response time was about 10 ns, chosen as a compromise between optimal time resolution and sensitivity. The signals induced in the coil were, after amplification, detected with a fast transient digitizer, limiting the bandwidth of the electronic detection circuitry to 200 MHz. In taking the spectra discussed in Sec. III the transient induction voltages were averaged by use of a gated integrator. In measuring the time evolutions of the magnetizations in Sec. IV, the signals were accumulated over typically 100 decays for the purpose of averaging.

The signals induced in the coil upon resonant optical pumping typically are 3 mV in height, which, given the characteristics of the coil and the excitation profile, corresponds to magnetization changes of about of 1.4×10^{17} μ_B cm^{-3}, or a concentration of excited Er^{3+} of $N^*\approx3\times10^{16}$ cm^{-3}. By comparing the energy required to achieve this N^* with the energy contained in a laser pulse, it is estimated that about 10% of the exciting light is absorbed by Er^{3+} centers. It is noted that N^* is subject to an uncertainty of, say, half an order of magnitude.

It should be noted that the induction voltages as measured contain a parasitic background, which needs to be corrected for prior to entering the analysis of Sec. IV. The undesired signals presumably originate from residual rf crossover and movements of the coil invoked by laser heating. The larger part of these signals was observed to be independent of the laser frequency, to scale with the laser intensity, and to increase linearly with the field. Their effects were estimated by bringing the laser out of resonance with the transition, and subsequently deducted. The smaller part appeared to be proportional with both the field and the optical absorption. It is removed by considering the signals remaining at such long times that all magnon-associated decays have died out.

III. PICKUP-COIL SPECTROSCOPY

In this section the method of detection of optical transitions with a pickup coil is applied to the case of the

$^4I_{15/2}(1)$-$^4F_{9/2}(1)$ transition of Er^{3+}, with emphasis on the assignment of the various components to the magnetic sublattices. To this end, the voltage induced in the coil has been measured as a function of the laser frequency. In its intensities, the spectrum thus obtained reflects, apart from the optical-absorption coefficients, the modifications associated with the transitions of the [001] components of the magnetic moments. As an example, the spectrum for an external field of 0.12 T along [001] is shown in Fig. 1(a), and compared with a conventional luminescence spectrum taken in the same field in Fig. 1(b). The positions of the four strongest lines in Fig. 1(a), two of which have inverted transition moments, indeed coincide with the transitions from the lower Zeeman component of $^4I_{15/2}(1)$ to the $^4F_{9/2}(1)$ doublet. These lines obviously are to be assigned to the two Er^{3+} sublattices according to their polarity and reflect in a quite direct way the antiferromagnetic order. The absolute line intensities differ between Er^{3+} on the two sublattices because the orientations of their magnetizations differ. The transverse components of the Er^{3+} magnetizations in fact rotate by $\pi/2$ about [001] when going from one sublattice to the other.[1] Indeed, the intensities are observed to vary as expected upon rotating the light polarization in the (001) plane. The weaker structures in Fig. 1(a) at longer wavelengths are the transitions associated with Er^{3+} raised out of the upper $^4I_{15/2}(1)$ doublet, whose population amounts to only 8% of the total ground-state population under the conditions used. These lines may similarly be assigned according to their polarity, however, with allowance for an overall sign reversal of the transition moments due to the Kramers symmetry.

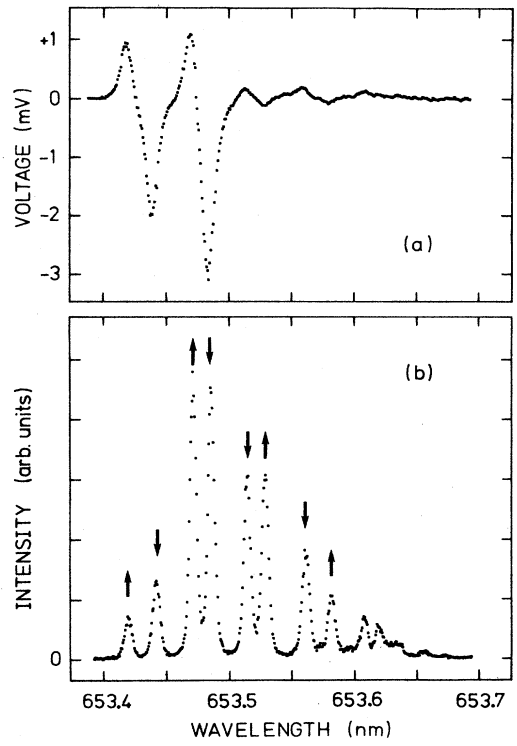

FIG. 1. Spectra of the $^4I_{15/2}(1)$-$^4F_{9/2}(1)$ transition of Er^{3+} at the two sublattices in an external field of 0.12 T along [001] at 1.5 K. (a) Spectrum acquired by monitoring the induction voltage while scanning the excitation frequency. (b) Luminescence spectrum upon excitation at 514 nm. Arrows indicate the assignment of the Zeeman components to the sublattices.

The assignment of the various components of the $^4F_{9/2}(1)$-$^4I_{15/2}(1)$ luminescence as established with coil detection is summarized in Fig. 1(b) with arrow markings. It is in conformity with the earlier assignment based on luminescence spectra,[1] where the distinction between the sublattices is accomplished by means of selective optical excitation. It is finally noted that fields of a few tenths of a T, such as used here, are sufficient to resolve the $^4I_{15/2}(1)$-$^4F_{9/2}(1)$ transitions pertaining to the two sublattices, but do not yet compensate the internal fields acting on the ill-directed Er^{3+}. These fields are approximately 0.5 T.[1] The induction voltages associated with the optical transitions starting from either one of the $^4I_{15/2}(1)$ levels indeed become of the same polarity when the field is raised above this value.

IV. TIME EVOLUTION OF OPTICALLY INDUCED MAGNETIZATIONS

A principal objective of this study is, on the one hand, to follow the spin-magnon relaxation as it increases upon moving away from the center of the Brillouin zone and, on the other hand, to determine the magnon damping. The selection of the magnon energies is accomplished by varying the splitting of the $^4F_{9/2}(1)$ doublet in relation to the $k=0$ magnon energy gap. A method to measure the spin-magnon relaxation, i.e., the lifetime of the $^4F_{9/2}(1)_+$ upper doublet level against emission of a resonant magnon in the decay to $^4F_{9/2}(1)_-$, is to compare the time evolutions of the magnetizations induced by selective optical excitation into $^4F_{9/2}(1)_+$ and $^4F_{9/2}(1)_-$. Here, the case of pumping into $^4F_{9/2}(1)_-$, for which the conditions are such that the optically induced magnetization remains steady within the time scale of the experiment, serves as a reference to eliminate the characteristics of the coil circuitry and the laser pulse. Because these may vary to some extent, the precaution has been taken to measure a $^4F_{9/2}(1)_-$ reference in conjunction with each $^4F_{9/2}(1)_+$ decay.

As an example of a $^4F_{9/2}(1)_-$ reference, we present the time evolution of the induction signal in zero magnetic field. Pulsed resonant excitation into $^4F_{9/2}(1)_-$ starting from the $^4I_{15/2}(1)_-$ ground state then typically gives rise to a signal of the shape as shown in Fig. 2. Also inserted in Fig. 2 is, independently measured immediately thereafter, the average envelope of the laser emission, which appears to contain secondaries of fluctuating amplitude. The induction signal given in Fig. 2 essentially is a convolution of the excitation profile and the pulse response of the circuit. Under the reasonable assumption of a single-exponential circuit response, the least-squares adjusted convolution is found to trace the data points to good agreement (solid line in Fig. 2). The circuit response time found is 10.8 ± 0.5 ns.

A selection of the induction signals observed upon optical excitation into $^4F_{9/2}(1)_+$ is presented in Fig. 3 after removal of the nonresonant contributions. In an external field along [001] of 3.03 T, i.e., below the field of 3.58 ± 0.05 T at which the $^4F_{9/2}(1)$ separation of Er^{3+} on the up sublattice equals the $k=0$ magnon gap,[1] the signal voltage remains positive, and essentially resembles the trace shown in Fig. 2. In fact, no difference in shape is observed with respect to the corresponding $^4F_{9/2}(1)_-$ trace. This is anticipated on the grounds of the smallness of the $^4F_{9/2}(1)$ splitting, inhibiting spin-magnon relaxation, and the slowness of the phonon-induced relaxation, occurring on a time scale of about 10 μs at 1.5 K in the field applied.[1] The upper two traces in Fig. 3 refer to fields along [001] of 4.03 and 5.19 T, corresponding to **k**'s about 5% and 10% out into the Brillouin zone, respectively. The negative tails appearing in these time evolutions clearly point to a decay of the magnetization following the initial buildup of magnetic moment during the laser pulse. It is thus seen that at 10% out in the zone the emission of magnons has become markedly faster than it is at 5%.

The data collected for the up-sublattice Er^{3+} have been analyzed in terms of rate equations to extract the decay time T_{1m} describing the relaxation among the $^4F_{9/2}(1)$ levels and the decay time τ_m of the magnons. The rate equations governing the time evolutions of the populations of Er^{3+} in the two $^4F_{9/2}(1)$ levels as well as the occupation number of the resonant magnons are taken identical to Eqs. (7) of Ref. 1. Upon restricting the magnon generation to the spontaneous part, and ignoring spin-phonon relaxation as well as decay back to the $^4I_{15/2}(1)$ ground state, evidently legitimate approximations here, these equations may be solved analytically to find for the time derivative of the [001] component of the optically induced macroscopic magnetization

$$\frac{dM^z(t)}{dt}=(\mu^z_+-\mu^z_g)\phi(t)+(\mu^z_--\mu^z_++\mu^z_m)T_{1m}^{-1}\int_0^t dt'\,\phi(t')\exp[-(t-t')/T_{1m}]$$
$$-\mu^z_m T_{1m}^{-1}\tau_m^{-1}\int_0^t dt'\int_0^{t'} dt''\,\phi(t'')\exp[-(t-t')/T_{1m}]\exp[-(t'-t'')/\tau_m]\ . \tag{1}$$

Here, $\mu^z_\pm$ are the expectation values of the magnetic moments of $^4F_{9/2}(1)_\pm$, μ^z_g similarly refers to the $^4I_{15/2}(1)_-$ ground state, μ^z_m is the magnetic moment carried by the magnons, and $\phi(t)$ is the excitation profile of the laser pulse normalized according to $\int_0^\infty \phi(t)dt=N^*$, with N^* the concentration of excited Er^{3+}. The signal voltage observed is then given by the convolution

$$V_+(t)=\int_0^t dt'\,R(t-t')\frac{d}{dt}M^z(t')\ , \tag{2}$$

in which $R(t)$ represents the response of the coil circuitry. As has already been pointed out, use is made of the reference traces with optical excitation into $^4F_{9/2}(1)_-$. In the latter case no relaxation occurs, and accordingly

$$V_-(t)=(\mu^z_--\mu^z_g)\int_0^t dt'\,R(t-t')\phi(t')\ . \tag{3}$$

Upon inserting Eq. (1), Eq. (2) acquires a form in which the convolution occurring in Eq. (3) may be factorized out. This enables us to simultaneously eliminate the shape of the excitation pulse $\phi(t)$ and the coil response function $R(t)$ by replacement with the measured quantity $V_-(t)$. We in fact arrive at

$$(\mu^z_--\mu^z_g)V_+(t)=(\mu^z_+-\mu^z_g)V_-(t)+(\mu^z_--\mu^z_++\mu^z_m)T_{1m}^{-1}\int_0^t dt'\,V_-(t')\exp[-(t-t')/T_{1m}]$$
$$-\mu^z_m T_{1m}^{-1}\tau_m^{-1}\int_0^t dt'\int_0^{t'} dt''\,V_-(t'')\exp[-(t-t')/T_{1m}]\exp[-(t'-t'')/\tau_m]\ . \tag{4}$$

The first term on the right-hand side in Eq. (4) arises from the initial change of the moment associated with feeding into $^4F_{9/2}(1)_+$, the second term results from the subsequent one-magnon decay to $^4F_{9/2}(1)_-$, and the last term reflects the removal of the magnons.

Equation (4) has been least-squares adjusted to coincidence with the data, with T_{1m} and τ_m as adjustable parameters. Here, the values $\mu^z_+=-\mu^z_-=-1.2\mu_B$ and $\mu^z_g=+5.6\mu_B$, derived from the Zeeman effect,[1] have been inserted for the Er^{3+} moments; for down magnons $\mu^z_m=+2.00\mu_B$. Further, T_{1m} being of the order of the response time of the coil and the duration of laser pulse, all convolutions have been carried out rigorously. The fits, represented by the solid lines in Fig. 3, appear to faithfully describe the observed traces. The minor noisy behavior in these lines, becoming apparent at times beyond 50 ns, is due to fluctuations propagated from $V_-(t)$. The values of τ_m resulting from the fits range from about 1 to 3 μs, but are not found to vary systematically with the wave vector. These long times are in conformity with the findings extracted from a bottlenecking experiment,[1] taken at 5% out into the zone, as well as antiferromagnetic resonance (AFMR) (Ref. 2) and parallel-pumping[3] experiments at the zone center. Note, however, that the present τ_m refer to escape out of the crystal rather than, as in Ref. 1, the optically pumped zone.

The fitted values of T_{1m}, the principal results of this study, are presented in Fig. 4 as a function of the magnon

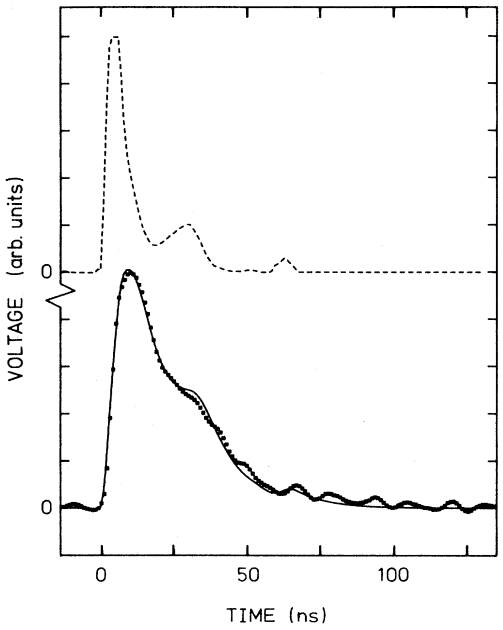

FIG. 2. Induction voltage upon optical excitation into $^4F_{9/2}(1)_-$ in zero magnetic field, serving as reference trace. Dashed line represents the profile of the exciting pulse. Solid line is a least-squares adjustment of the excitation pulse convoluted with the circuit response.

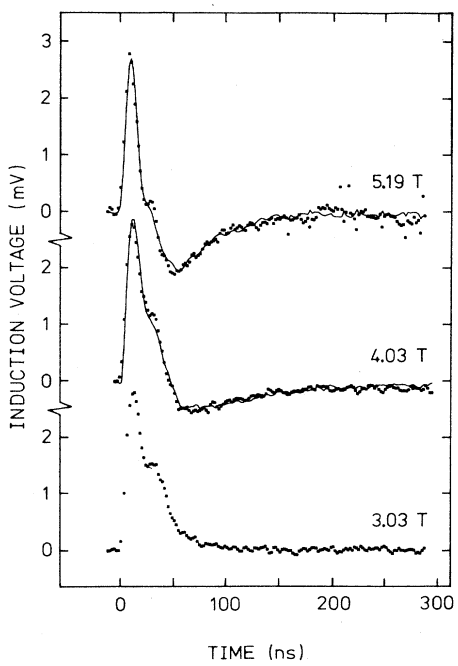

FIG. 3. Induction signals following optical excitation into $^4F_{9/2}(1)_+$ for fields along [001], as indicated. Solid lines are fits to the traces taken beyond intersection with the down-magnon branch.

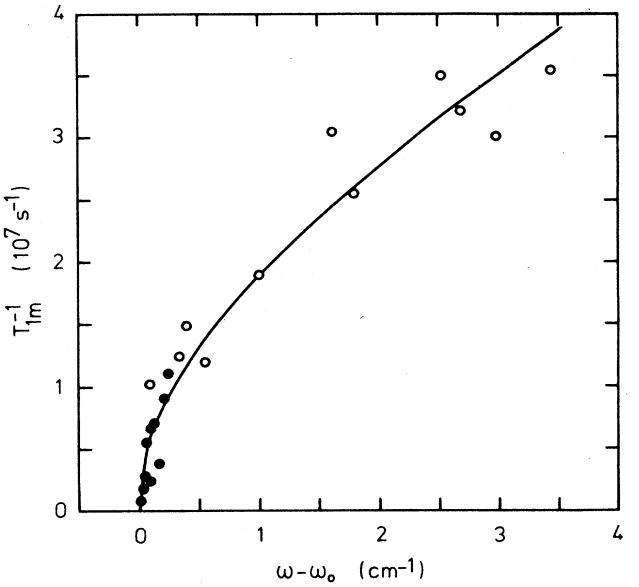

FIG. 4. Dependence of T_{1m}^{-1} vs the magnon energy ω relative to $\omega_{k=0}$. Open circles are data obtained with coil detection, while closed circles are from optically detected decays (Ref. 1). Solid line represents the dependence of T_{1m}^{-1} on ω according to Eq. (6).

energy relative to $k=0$, with the field as parameter. It has been verified by a number of experiments at N^* reduced by factors 2 and 4 that these results are not noticeably affected by reabsorption of magnons in the pumped zone. We recall that the maximum field attained corresponds to **k**'s 10% out into the zone. In Fig. 4 further are inserted, as closed circles, analogous results derived from optically detected spin-magnon decays within $^4F_{9/2}(1)$.[1] The course of the spin-magnon relaxation rate is seen to exhibit a steep rise at the bottom of the magnon band, going over into a gradually diminishing increase towards higher energies. At $\hbar(\omega-\omega_0)\approx 3.5$ cm^{-1}, T_{1m}^{-1} has risen to 4×10^7 s^{-1}. The dependence of T_{1m}^{-1} on $\omega-\omega_0$ in fact very much resembles the square-root dependence characteristic of the density of states in the quadratic regime. This will be given a more firm basis in Sec. V below.

With regard to Er^{3+} on the down sublattice, it is noted briefly that the induction signals observed upon pumping into $^4F_{9/2}(1)_+$ are entirely similar to those pertaining to the up-sublattice case, both in shape and polarity. The crossing of the $^4F_{9/2}(1)$ splitting with the $k=0$ magnon gap here occurs at 4.60 ± 0.05 T. This field easily overcompensates the downwards directed internal field (cf. Sec. III). The spin-magnon times derived from induction signals, not presented in detail here, do not markedly deviate from those in Fig. 4.

V. SPIN-MAGNON RELAXATION

To discuss the observed dependence of T_{1m}^{-1} on the magnon energy, we calculate the spontaneous rate of the $^4F_{9/2}(1)_+$-$^4F_{9/2}(1)_-$ transition against emission of a reso-

nant magnon for an isolated Er^{3+} center subject to an interaction of general form with the Mn^{2+} surrounding it. The calculation relies on time-dependent perturbation theory to first order. The interaction Hamiltonian quite generally reads

$$\mathcal{H}_{\text{Er-Mn}}=\sum_{\delta}\sum_{\mu,\nu} j_{\mu\nu}J'_{\mu}S_{\nu}(\delta)\ , \tag{5}$$

where $\mathbf{J}'$ is the effective angular momentum of an up-sublattice Er^{3+}, $\mathbf{S}$ is the spin of the Mn^{2+} displaced by δ, and μ and ν running over x, y, and z. The coefficients $j_{\mu\nu}$ specify the strength of the interaction. Equation (5) is given a form such as to contain diagonal and off-diagonal exchange. We have chosen to treat the Er^{3+} with an effective J' on the grounds that the next higher doublet is at a distance of 50 cm^{-1} compared to doublet splittings of order 1 cm^{-1}. The crystal field is of such low symmetry that all M_J components of the parent state $^4F_{9/2}$ are admixed into $^4F_{9/2}(1)$.[4] The coefficients of admixture are unknown and therefore absorbed in the $j_{\mu\nu}$. They further depend on whether $\mathbf{J}'$ is to be associated with the Er^{3+} spins, as is the case for exchange interactions, or rather with the magnetic moment operator, as is the case for dipolar interactions. For simplicity, we restrict the summation over δ to the nearest neighbors on the opposite sublattice ($z=8$), and further assume the $j_{\mu\nu}$ independent of δ.

We proceed, in the standard way,[5] with Holstein-Primakoff transformation converting $\mathbf{S}$ into local spin-deviation operators, Fourier decomposition to sublattice-confined spin waves, and finally Bogoliubov transformation to the magnon operators $\alpha_{\mathbf{k}}^{\dagger}$, $\alpha_{\mathbf{k}}$, $\beta_{\mathbf{k}}^{\dagger}$, and $\beta_{\mathbf{k}}$ creating and annihilating linearized excitations out of the antiferromagnetic ground state. The α and β magnons chiefly reside on the up and down sublattices, respectively. As concerns the Er^{3+}, we observe that the applied field dominates the transverse internal field to the extent that the Er^{3+} moments are aligned along [001] to within 5°. We, therefore, adopt [001] as the quantization axis. We define the local operators a and $a^{\dagger}$, inducing transitions from $^4F_{9/2}(1)_+$ to $^4F_{9/2}(1)_-$ and vice versa, respectively, through $J'^{-}=(2J')^{1/2}a$ and $J'^{+}=(2J')^{1/2}a^{\dagger}$. The one-magnon part of $\mathcal{H}_{\text{Er-Mn}}$ then becomes

$$\mathcal{H}_{\text{Er-Mn}}=z\left[\frac{J'S}{N}\right]^{1/2}\sum_{\mathbf{k}}\gamma_{\mathbf{k}}(M_1 v_{\mathbf{k}}a\alpha_{\mathbf{k}}^{\dagger}+M_2 u_{\mathbf{k}}a\beta_{\mathbf{k}}^{\dagger}+\text{c.c.})\ , \tag{6}$$

where

$$M_1=(j_{xx}+j_{yy})+i(j_{yx}-j_{xy})\ ,$$

$$M_2=(j_{xx}-j_{yy})+i(j_{yx}+j_{xy})\ ,$$

and

$$\gamma_{\mathbf{k}}=z^{-1}\sum_{\mathbf{k}}\exp(i\mathbf{k}\cdot\delta)$$

is a geometrical summation. The Bogoliubiov coefficients $u_{\mathbf{k}}$ and $v_{\mathbf{k}}$ pertaining to the spin-wave band are given by

$$u_{\mathbf{k}}^2=\tfrac{1}{2}\{(1+\alpha)/[(1+\alpha)^2-\gamma_{\mathbf{k}}^2]^{1/2}+1\}\ ,$$
$$v_{\mathbf{k}}^2=\tfrac{1}{2}\{(1+\alpha)/[(1+\alpha)^2-\gamma_{\mathbf{k}}^2]^{1/2}-1\}\ , \tag{7}$$

with $\alpha=0.016$ the anisotropy parameter appropriate to MnF_2.[6]

By energy conservation, in the experiment only down magnons are excited. The spontaneous relaxation rate against creation of a down magnon derived from Eq. (6) reads

$$T_{1m}^{-1}=\frac{2\pi z^2J'S}{\hbar^2N}\gamma_{\omega}^2|M_2|^2u_{\omega}^2D(\omega)\ , \tag{8}$$

where it is noted that $\gamma_{\mathbf{k}}$ and $u_{\mathbf{k}}$ have unique values γ_{ω} and u_{ω} at a surface in the Brillouin zone of constant magnon energy $\hbar\omega-2\mu_BH$, as selected by the $^4F_{9/2}(1)$ level separation Δ. The quantity $D(\omega)$ is the magnon density of states, which in the quadratic approximation equals, per branch,

$$D(\omega)=\frac{4N}{\pi^2}\frac{\omega(\omega^2-\omega_0^2)^{1/2}}{\omega_E^3}\ , \tag{9}$$

where ω is the zero-field angular frequency of the down magnons. For MnF_2, $\omega_0=8.71\pm0.04$ cm^{-1} and $\omega_E=48.8$ cm^{-1}.[6] For Er^{3+} located at the down sublattice, expressions similar to Eqs. (6) and (8) hold, except for mutual replacement of the Bogoliubov coefficients.

When comparing the results calculated from Eq. (8) with experiment, it emerges that Eq. (8) traces the data points in Fig. 4 over the entire range of magnon energies considered (solid line in Fig. 4). The comparison yields $|M_2|=0.042\pm0.004$ cm^{-1}. It is noted that the dependence on ω is predominantly contained in the density of states, the combination $\gamma_{\omega}^2u_{\omega}^2$ diminishing towards higher ω by 10% only.

It is of interest at this point to consider the nature of the spin-magnon relaxation in somewhat greater detail. First, apart from not conserving $\mathbf{k}$, the process does not conserve angular momentum. In the decay of Er^{3+} a magnetic moment $g\mu_B$ with $g=2.4$ is generated along [001]. With a Landé factor of $g_J=\frac{4}{3}$, this corresponds to an angular momentum of $-g/g_J=-1.8\hbar$. The subsequently emitted down magnon carries a magnetic moment of $2\mu_B$, corresponding to an angular momentum of $-\hbar$. Both the decay of Er^{3+} and the generation of a down magnon accordingly involve the creation of a downward angular momentum along [001]. This implies that the Er-Mn interaction must be non-Heisenberg in character. In the formalism this is expressed by the fact that M_2 vanishes in case of isotropy of the interaction. As to the origin of M_2, its magnitude suggests dipolar interactions to be a candidate. The zz component of the dipolar tensor may be derived from the anisotropy field $H_A=0.85$ T, to be $\frac{2}{3}H_A=0.56$ T when expressed as a field acting on Er^{3+}. This would yield estimates for the interaction parameter $j_{\mu\nu}$ of order $\frac{2}{3}g\mu_BH_A/z=0.08$ cm^{-1}. On the other hand, the combination of $j_{\mu\nu}$ making M_2 vanishes for dipolar interactions, at least for $k=0$,

when Er^{3+} is situated on a lattice position having tetragonal symmetry. Therefore, given that the Er^{3+} are known to be displaced from such positions,[1] dipolar spin-magnon relaxation is not unlikely to contribute to some extent. Another candidate, of course, remains Er-Mn exchange. Precise values of the Er^{3+}-Mn^{2+} exchange in MnF_2 are not available, but $4f$-$3d$ exchange interaction by mediation of F^- generally is of order 0.1 cm^{-1}. The fact that the effective internal fields acting on the Er^{3+} in $^4F_{9/2}(1)$ differ from those experienced by Er^{3+} in $^4I_{15/2}(1)$ indicates that a significant contribution arises from exchange.

A final note concerns local modes. The Er^{3+}-Mn^{2+} interaction being smaller than the intrahost interaction by an order of magnitude, Er^{3+} is quite near to magnetic vacancy. Still, the associated disturbance has died out beyond a few shells of neighbors.[7] The modes affected are all well above the band bottom, except for the occurrence of a single s mode with an energy in the band gap residing on the Er^{3+} itself. The paucity of the impurity modes at the Er^{3+} concentration used, however, minimizes their effects.

VI. CONCLUSIONS

Optical excitation of Er^{3+} has been used to generate magnons in antiferromagnetic MnF_2 with **k**'s up to about 10% towards the zone boundary. The magnons are detected via the voltage the associated magnetization induces in a pickup coil. The magnons generated appear to live as long as 1 μs, which evidently is related to the pure spin character of spin waves in Mn^{2+} systems. The emission of magnons by Er^{3+} typically takes place within about 100 ns, and in the reach of **k** considered its rate approximately scales with the density of states, indicating near constancy of the relaxation per magnon mode.

ACKNOWLEDGMENTS

The authors thank C. R. de Kok and F. W. M. Wollenberg for technical assistance. The work was made possible by a grant from the Netherlands Foundation Janivo, and further was financially supported by the Netherlands Foundation Fundamenteel Onderzoek der Materie (FOM) and the Nederlandse Organisatie voor Wetenschappelijk Onderzoek (NWO).

[1]G. J. Jongerden, A. F. M. Arts, J. I. Dijkhuis, and H. W. de Wijn, Phys. Rev. B **38**, 4372 (1988).

[2]J. P. Kotthaus and V. Jaccarino, Phys. Rev. Lett. **28**, 1649 (1972).

[3]J. Barak, S. M. Rezende, A. R. King, and V. Jaccarino, Phys. Rev. B **21**, 3015 (1980).

[4]G. H. Dieke, *Spectra and Energy Levels of Rare Earth Ions in Crystals* (Interscience, New York, 1968), Chap. 11.

[5]F. Keffer, in *Encyclopedia of Physics,* edited by S. Flügge (Springer, New York, 1966), Vol. XVIII, Part II.

[6]F. M. Johnson and A. H. Nethercot, Jr., Phys. Rev. **114**, 705 (1959); C. Trapp and J. W. Stout, Phys. Rev. Lett. **10**, 157 (1963); see also Ref. 5.

[7]M. Butler, V. Jaccarino, N. Kaplan, and H. J. Guggenheim, Phys. Rev. B **1**, 3058 (1970); L. R. Walker, B. C. Chambers, D. Hone, and H. Callen, *ibid.* **5**, 1144 (1972); J. A. van Luijk, A. F. M. Arts, and H. W. de Wijn, *ibid.* **21**, 1963 (1980); H. van der Vlist, A. F. M. Arts, and H. W. de Wijn, *ibid.* **30**, 5270 (1984).